Desalination and Water Treatment
www.deswater.com

doi: 10.5004/dwt.2021.26536

209 (2021) 392–401
January

Comparative adsorptive and kinetic study on the removal of Malachite Green in aqueous solution using titanium coated graphite and titanium coated graphite with CNT-ABS nanocomposite

Usha Jinendra[a,†], B.M. Nagabhushana[b,*,†], Dinesh Bilehal[a,†]

[a]*P.G. Department of Chemistry, REVA University, Katigenahalli, Yalhanka, Bangalore 560064, India, emails: ushajinendra@gmail.com (U. Jinendra), drbilehal@gmail.com (D. Bilehal)*
[b]*Department of Chemistry, M S Ramaiah Institute of Technology, Bangalore 560054, India, email: bmnshan@yahoo.com (B.M. Nagabhushana)*

Received 11 November 2019; Accepted 31 August 2020

ABSTRACT

The titanium was coated on graphite using the electroless method. The titanium coated graphite nanoparticle was modified with CNT-ABS nanocomposite by a sequence of steps, that is, sensitizing, activating, and coating with prior cleaning step. The titanium coated graphite with and without CNT-ABS nanocomposite was characterized by using X-ray diffraction, Fourier transform infrared spectroscopy, scanning electron microscopy, and transmission electron microscopy. The dye absorption efficiency is checked with and without nanocomposite of CNT-ABS. Malachite green dye was used as organic toxic waste. It was observed that Malachite green dye absorption efficiency of titanium coated graphite with CNT-ABS composite was better than without. The effect of adsorbent dosage (0.6 g/L), initial dye concentration (10 mg/L), pH (6), and contact time (60 min) was evaluated. The equilibrium concentration and the adsorption capacity were evaluated using three different models namely Langmuir, Freundlich, and Tempkin isotherms. The kinetic study determined that Malachite green dye adsorption was in good analogy with the pseudo-first-order kinetic model.

Keywords: Malachite green dye; CNT-ABS nanocomposite; SEM; TEM; XRD; Adsorption

1. Introduction

The textile industries are the highest generators of liquid effluent since the huge quantity of water is used in the dying process [1]. Synthetic dyes are being used in a wide range of products such as clothes, leather accessories, furniture, and food industries. About 10%–15% of the dyes used, released through the effluent process [2]. Its presence in natural rivers and streams can cause harm to aquatic life due to its toxic nature. Many of the dyes are non-biodegradable and also carcinogenic [3]. Presently, there are greater than 9,000 different dyes which are used in color index belonging to several chemical application classes. A number of these physical and chemical treatment processes including adsorption, precipitation, air stripping, reverse osmosis, flocculation, and ultrafiltration are often employed to remove these deadly pollutants from water. Almost all of these methods suffer from a number of drawbacks [4]. A carbon nanotube (CNT) has tunable chemical, physical, electrical, and structural properties, excite groundbreaking technologies to address the water pollution problems. CNT based nanotechnologies are used in many fields, such as catalyst, filters, sorbents, or membranes [5]. Electron–hole pairs that are created will react with oxygen and water

* Corresponding author.

† Present address: Karnataka University, Dharwad

molecules to form superoxide anions and hydroxide radicals which increase oxidizing power and thereby to be used in many industrial dye compounds [6–9]. CNT-ABS nanotubes are carbon-based nanotubes which have multi-walled carbon nanotubes dispersed in ABS by unique hollow tube structure [10]. CNTs and CNT-ABSs have been projected for different applications such as hydrogen storage devices, sensors, and many more [11]. The electroless technique is perhaps the most promising because it does not need external electrical supply, in order to complete the deposition. The presence of a chemical reducing agent in the solution is used on the different substrates to generate assisted deposition.

Carbons materials and its modified surfaces area and large surface areas, extensive trials have been conducted on the adsorption of Malachite green dye [12]. Malachite green is an organic dyestuff compound (Fig. 1), is chlorite salt of $[C_6H_5C(C_6H_4N(CH_3)_2)_2]$. It traditionally serves as a coloring agent for silk, linen, paper, jute, cotton, and leather as a coloring additive. Malachite green is known to be a triarylmethane colorant and is used in the dyestuff industry.

In the present paper, Malachite green dye was selected as the typical organic dye to investigate adsorption kinetics of pollutant on the titanium coated graphite CNT-ABS nanocomposite and titanium coated graphite under different experimental conditions. The kinetic data was investigated on different models were adopted to fit the experimental data. This may be applicable to practical applications of the adsorbent during wastewater treatment.

2. Materials and methods

Malachite green dye ($C_{23}H_{25}N_2$) (ARGrade 99% pure, Merck) and graphite (ARGrade 99% pure, Merck, Particle size (<50 μm)), was used without further purification, hydrochloric acid (HCl) (ARGrade 99% pure, Merck), Tin(II) chloride ($SnCl_2$) (ARGrade 99%pure, Merck), silver nitrate ($AgNO_3$) (ARGrade 99% pure, Merck), titanium chloride ($TiCl_4$) (ARGrade 99% pure, Merck), sulfuric acid (H_2SO_4) (ARGrade 98% pure, Merck), sodium citrate ($Na_3C_6H_5O_7$) (ARGrade 99% pure, Merck), NaOH pellets (ARGrade 99% pure, Merck), and hydrazine (ARGrade 99% pure, Merck) and CNT (ARGrade, name NC7000™ were supplied by Nanocyl S.A. Sambreville, Belgium) were used in this experiment. The technical data sheet says CNT has an average diameter of 9.5 nm, average length of 1.5 μm, and a surface area of 250–300 m^2/g, ABS (ARGrade 99% pure, and trade name Sinkral®F322). The double distilled water obtained from the lab were used throughout this study.

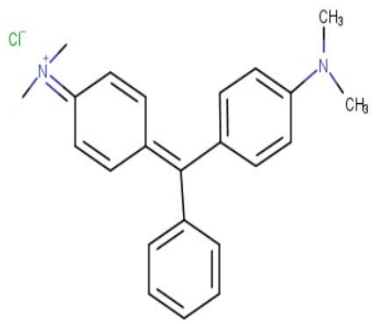

Fig. 1. Schematic structure of malachite green.

2.1. Experimental

2.1.1. Electroless coating of titanium on graphite

Titanium coated on graphite using an electroless method. The process of coating relies on a particular order which follow with sensitizing, activation, coating, and drying stages are included, which is broadly divided into three different steps:

- *Step* 1: *Sensitizing*: the graphite was sensitized by treatment which was carried out in 200 mL of a solution containing 10 g of tin(II) chloride ($SnCl_2$) and 2 mL of hydrochloric acid for 15–30 mins. Then the sensitized graphite was rinsed in distilled water.
- *Step* 2: *Activation*: the obtained graphite was transferred to activating 200 mL solution containing 0.5 g of silver nitrate because to increase the activity of carbonation and 2 mL of hydrochloric acid and stirred for 15–30 mins. The activated graphite is rinsed in distilled water.
- *Step* 3: *Coating*: the activated graphite was transferred to the bath containing 5 g of titanium chloride and 5 g of sulfuric acid along with distilled water. Five grams of sodium citrate, 5 g of NaOH pellets, and 5 mL of hydrazine was added and mixed using mechanical stirrer and allowed for a day and it is filtered.

2.1.2. Preparation of titanium coated graphite-CNT ABS composite

The obtained titanium coated graphite was further divided into two equal part, in which one is used as the same and second half is further mixed with the CNT-ABS nanotubes by grinding the CNT-ABS nanotubes to fine powder (1 g) is weighed and mixed with 10 g of titanium on graphite using the stirrer by adding little of 2 mL of hydrochloric acid and allowed for a day so that, the compounds are completely dispersed. The schematic representation of titanium coated graphite-CNT ABS composite is shown in flow chart of Fig. 2. The titanium coated graphite without CNT-ABS and with CNT-ABS nanotubes were rinsed multiple times in distilled water and dried in a hot air oven and sent for characterization.

2.1.3. Adsorption study

The batch analysis was carried out to find out the adsorption of dyes onto the adsorbent in 250 mL glass flasks which contain a certain volume of fixed initial concentrations of dye solution and known amount of adsorbent. The flasks were kept on a magnetic stirrer at a speed of 500 rpm. At fixed time intervals, the sample solutions were filtered after attaining equilibrium using Whatman filter paper and residual concentrations were determined. The adsorbate concentrations in the initial and final solutions were calculated by using UV-vis spectrophotometer (Perkin-Elmer Lambda 25 spectrophotometer, USA) at 621 nm (λ_{max}). The amount of Malachite green adsorbed on titanium coated graphite CNT-ABS nanocomposite

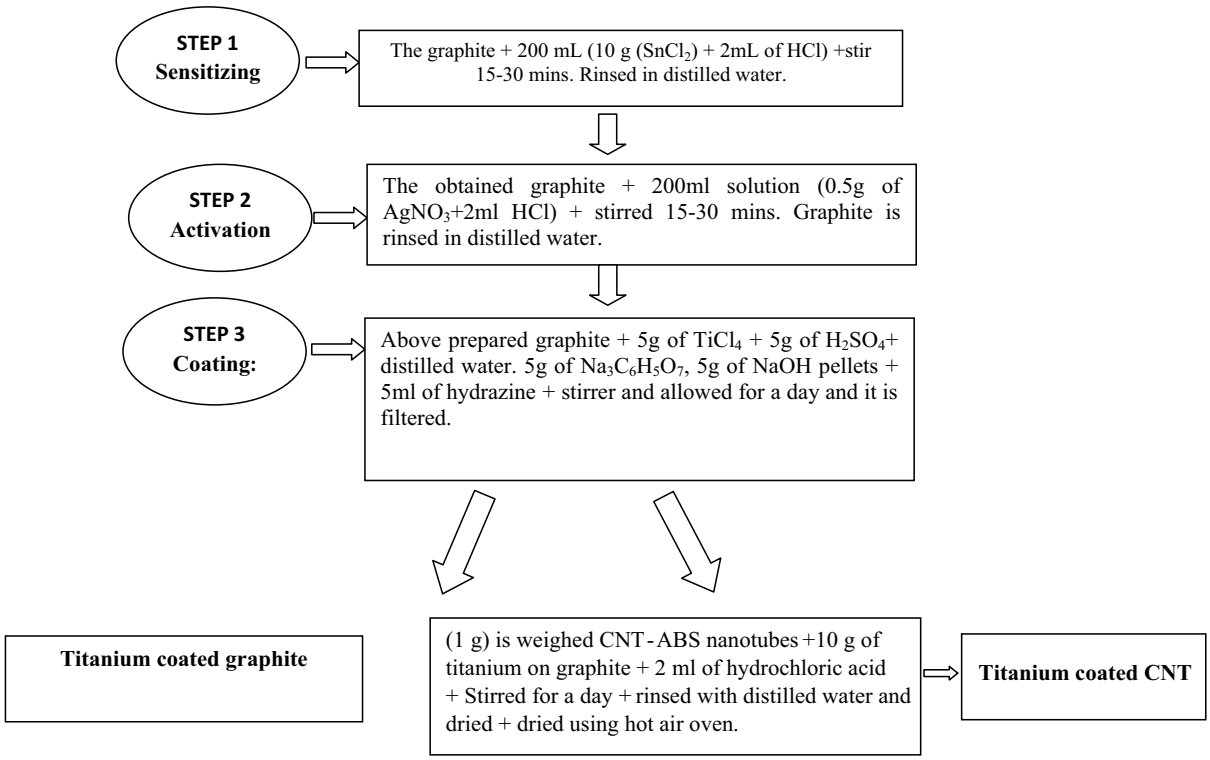

Fig. 2. Schematic flow chart of the preparation of titanium coated graphite-CNT ABS composite.

and titanium coated graphite was calculated from the difference between the initial concentration and the equilibrium one. The adsorption percentage was derived from the difference of the concentration before adsorption (C_0) and the concentration after adsorption (C_e).

$$\text{Adsorption } \% = \frac{\left(C_0 - C_e\right)}{C_0} \times 100 \quad (1)$$

2.2. Characterization of the titanium coated graphite and titanium coated graphite CNT-ABS nanocomposite as an adsorbent

2.2.1. X-ray diffraction

It is observed that titanium coated graphite CNT-ABS nanocomposite shows a good crystalline phase compared to titanium coated graphite. Where in the above Fig. 3, titanium coated graphite CNT-ABS nanocomposite pattern of XRD shows a well-known different characteristic diffraction peaks, and also it has matched well with JCPDS file of titanium on graphite with CNT-ABS is 00-2088. The XRD pattern (Fig. 3b) of the titanium on graphite adsorbents show typical pattern and is little amorphous in nature without clear characteristic peaks having main peaks at 2θ at 26°, 36°, 44° and 54° were and matched well as JCPDS file of titanium on graphite is 29-0661.

2.2.2. SEM and TEM analysis

The SEM image (Fig. 4I (a)) of the sample titanium graphite with CNT-ABS were observed to be a roughly spherical shape. It can be seen that the particle sizes of samples are in the ranges from 53.0 to 78.0 nm were observed. Whereas, the SEM image of titanium on graphite is not clear (Fig. 4I (b)) and the particle sizes were not clearly observed since the particle size is very small. Fig. 4II (c–h) show the typical high-resolution TEM image of a coating of titanium on graphite with CNT-ABS and without CNT-ABS nanocomposite. It confirms that the titanium on graphite nanoparticles have an irregular small spherical structure in both with and without nanocomposite, as it can be seen from the image. By carefully observing the TEM image proves it has a spherical structure [13]. The average diameter of the Titanium on graphite nanoparticles has spherical structure with particle size about 44–55 nm. In addition to this, no nanoparticle aggregation is found on the surface of the graphite since ABS polymer is used for the dispersibility of titanium on graphite NPs. Moreover, the TEM image was shown an ABS polymer layer surrounding around of nanoparticles that was prohibited the particles agglomeration and established the effective surface coating. In conclusion, titanium coated on graphite has 44–55 nm size, and titanium graphite with CNT-ABS has 53.0–78.0 nm which is due to the hollow structure of CNT and causes better adsorption.

2.2.3. FTIR analysis

Fourier transform infrared spectroscopy (FTIR) (Fig. 5) is used to identify the adsorbed dye on the surface of the adsorbent before and after the dye adsorption. There is no change in the FTIR spectra of titanium coated graphite

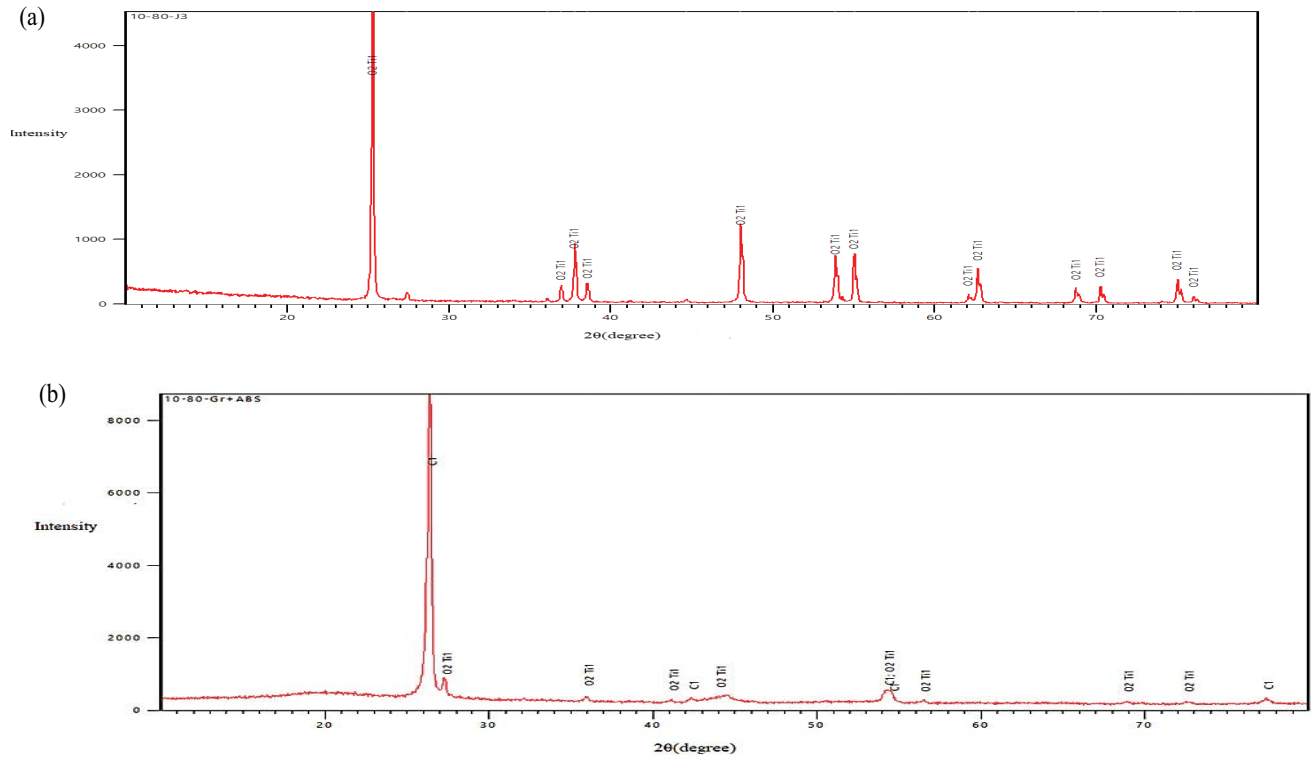

Fig. 3. XRD pattern of (a) titanium coated graphite CNT-ABS nanocomposite and (b) titanium coated graphite.

before and after the adsorption. Since the mass of the dye adsorption is in less quantity on titanium coated graphite and the sensitivity of the FTIR instrument is more, it will not be able to detect the adsorption in the FTIR. While, the spectra of titanium coated graphite CNT-ABS nanocomposite indicate intensive bands at 3,400; 3,500; and 3,600 cm^{-1} shows the presence of hydroxyl functional of CNT (surface adsorbed). After adsorption of titanium coated graphite CNT-ABS nanocomposite bands in 1,780; 1,750 (C=O stretch); and 1,690 (C=C stretch) mainly due to the adsorption of malachite green dye. Since the surface area in more in the CNT due to hollow structure, the amount of adsorption is more and there is a band of malachite green is observed in infra-red spectra due to adsorption of malachite green dye.

2.3. Effect of adsorbent dosage

The mass adsorbed was studied with the different mass of titanium graphite with CNT-ABS and titanium graphite on malachite green dye absorption, 10 mg/L dye concentration for 60 min. Fig. 6 reveals that, the effect of adsorbent dosage on dye removal of titanium on graphite with CNT-ABS, and it is found 90% absorbance, whereas titanium on graphite shows only 36% absorbance. Because the adsorptive capacity of titanium on graphite available was not fully utilized and the adsorption of molecules is likely to occur around molecules that are already present (occupied) on the surface. With CNT-ABS the surface area is more and the adsorptive capacity is more because it contains CNT, which contributes to more surface area.

2.4. Effect of pH

The pH of a solution is one of the important parameters in the adsorption process. During this study, it reveals that the adsorption of dye was dependent on the pH. The effect of pH on adsorption of dye onto the titanium coated graphite and titanium coated graphite CNT-ABS nanocomposite was studied in the pH range 1–12 (Fig. 7) and the maximum dye removal capacity was observed at pH 6 for titanium coated graphite with CNT-ABS. Further increase in pH, no significant change in dye removal is observed. Titanium coated graphite CNT-ABS nanocomposite has favored in the removal of the dye malachite green due to the electrostatic interaction increased the adsorption and shows stable in the pH range 6–12 due to hydrogen bonding, that is, repulsion of H^+ ion with the cationic dye molecules decreases the adsorption and shows constant adsorption. Hence, the surface will then exhibit a cation exchange capacity [14].

2.5. Effect of contact time

As given in Fig. 8, % of adsorption value improves with the increase in the contact time from 10 to 60 mins. The adsorption capacity of titanium coated graphite CNT-ABS nanocomposite increased with the increase in time. The subsequent constant adsorption process maybe because of vacant surface sites may be exhausted [15]. It is observed that, titanium coated graphite CNT-ABS nanocomposite shows far better adsorbance compared to titanium on graphite. Due to high interconnected pore

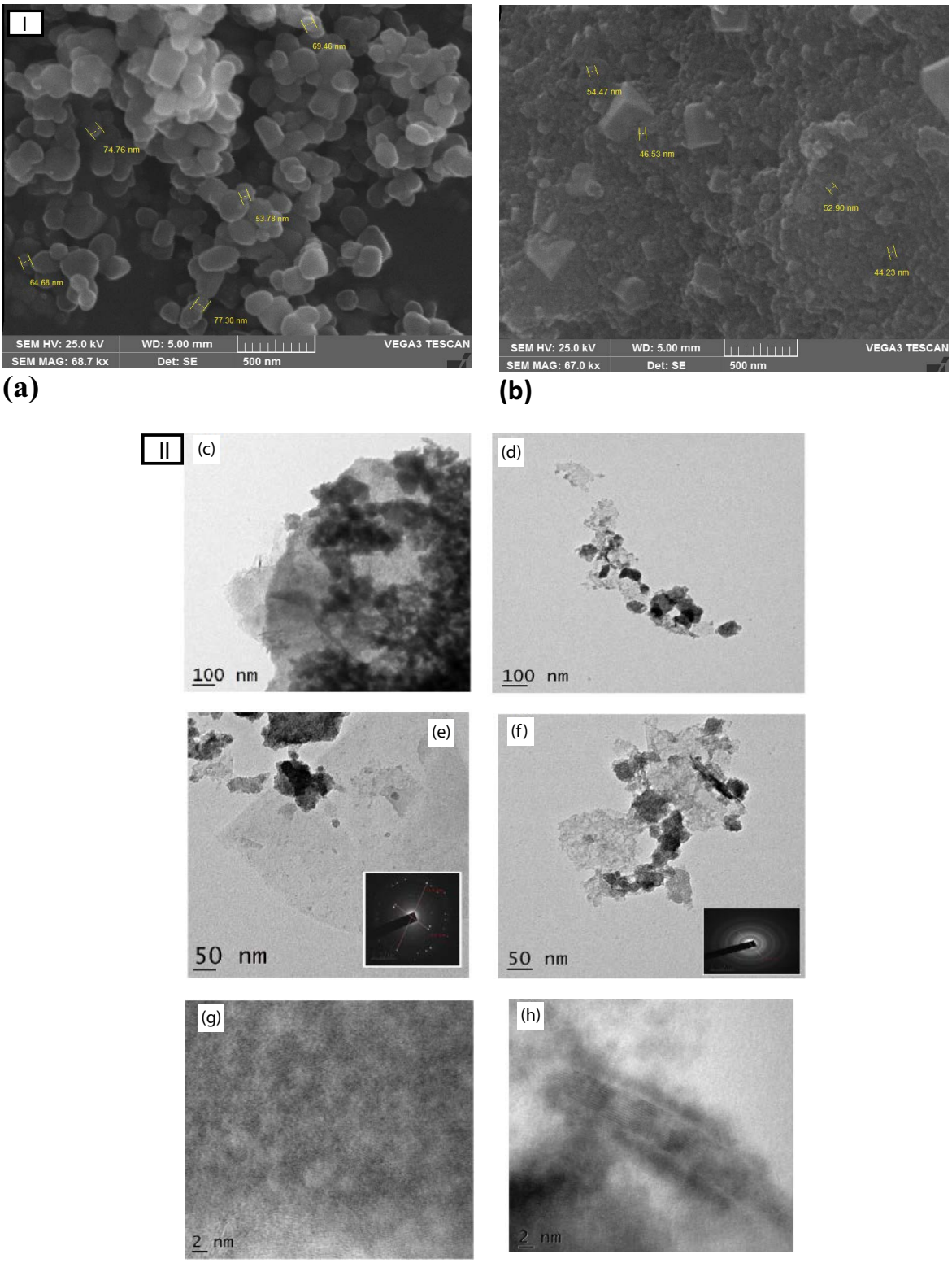

Fig. 4. (I) SEM and (II) TEM analysis image of (c,e,g) titanium coated graphite and (d,f,h) titanium coated graphite CNT-ABS nanocomposite.

structure and less pore deformation compared to titanium on graphite, as time advances the surface coverage on the adsorbent is high, after that no adsorption takes place and becomes a constant. Compared to bimetallic nanoparticle Fe–Cu nanoparticles (dosage 10 mg/L) and Graphene oxide/cellulose beads (dosage 10 mg/L) with malachite green dye which has more contact time of 20–24 h, respectively [12,16]. Our work, titanium coated graphite CNT-ABS

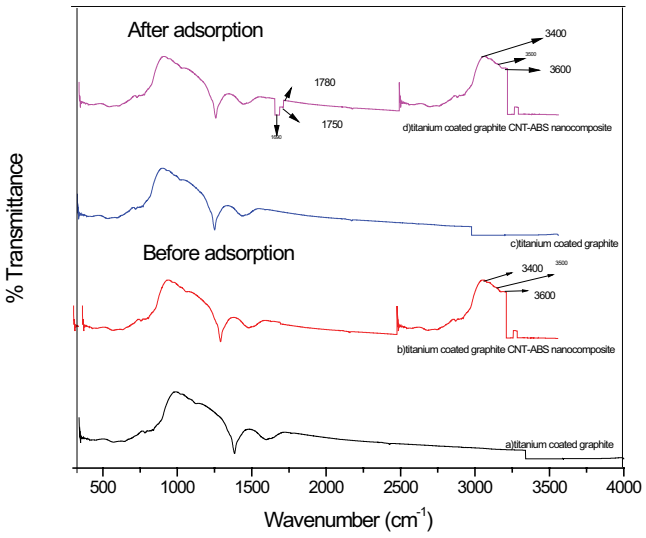

Fig. 5. FTIR spectra before adsorption (a) titanium coated graphite, (b) titanium coated graphite with CNT-ABS nanocomposite, (c) titanium coated graphite after adsorption, and (d) titanium coated graphite with CNT-ABS nanocomposite after adsorption.

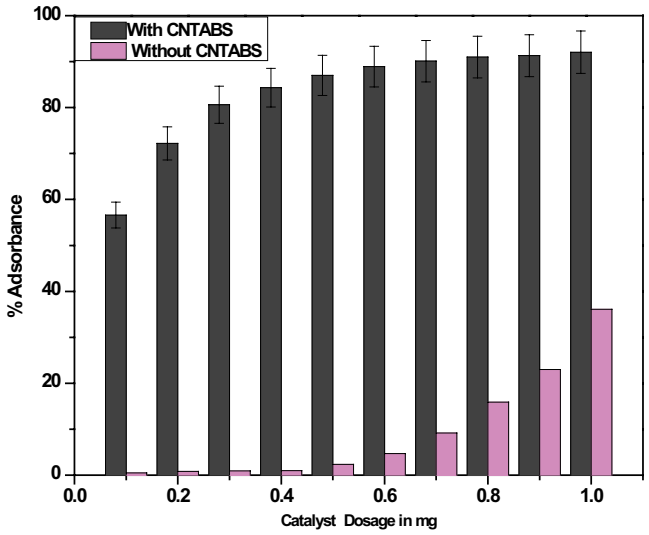

Fig. 6. Effect of dosage on malachite green dye adsorption.

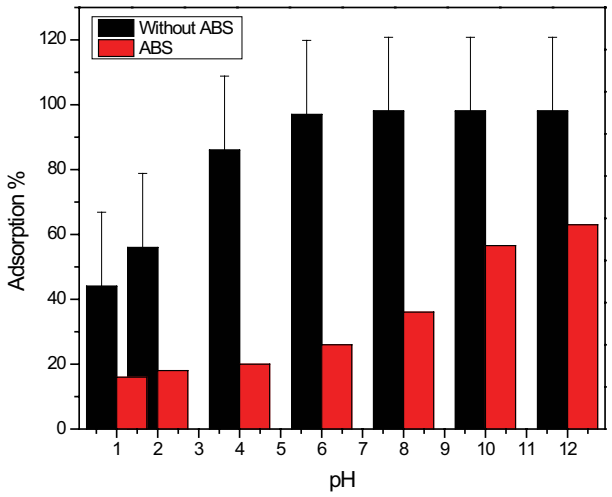

Fig. 7. Effect of pH on malachite green dye adsorption.

nanocomposite shows better adsorption capacity and less contact time of 1 h (60 min) due to large surface of CNT.

2.6. Effect of initial concentration

The effect of the initial concentration of malachite green dye in the solution was investigated and shown in Fig. 9. The investigation was conducted with fixed adsorbent dosage (10 mg), at constant pH (6), contact time (60 min) conditions. The percentage of adsorption decrease with increase in initial dye concentration. The initial adsorption capacity was 94%. Here also, titanium coated graphite with CNT-ABS nanocomposite shows far better adsorbance compared to titanium coated graphite. Because of the autocatalytic activity of the titanium coating on the graphite with CNT-ABS has more bundle walled nanotube, which is expected to have a greater influence on the adsorption of organic pollutant malachite green dye. The adsorption of malachite green dye depends especially on the CNT-ABS due to a specific interaction between the malachite green dye adsorption and the functional groups of CNT-ABS that favorable the malachite green dye adsorption. The percentage of adsorption decrease may be due to adsorption sites gets saturated resulting in a decrease in the available surface area for the malachite green dye [17].

2.7. Zero-point charge

The evaluation of surface properties is very important for any new material before starting for adsorption studies. In an attempt, to study the surface charge of the synthesized material, pH drift method was done using 0.01 N NaOH. In a series of solutions of NaOH added a small amount of nanocrystalline titanium coated graphite with CNT-ABS and the initial pH of each solutions was adjusted between 2 and 12 using 0.01 N HCl and 0.01 N NaOH. All these mixtures were kept shaking for 10 h to reach equilibrium and the final pH was noted. Zero-point energy of titanium coated graphite with CNT-ABS as found to be 6.0 (Fig. 10) which signifies that below this value the titanium coated graphite with CNT-ABS nanoparticle is positively charged might be due to protonation and above 6.0 has a negative charge.

2.8. Adsorption isotherm

The adsorption isotherm is important to design adsorption systems. The mechanism of adsorbent was studied by isotherm models. The mathematical relation between dye concentration and the mass of the dye adsorbed at a particular time, dosage, and pH is given by the adsorption isotherms. Langmuir, Freundlich's, and Temkin models are amongst explaining solid–liquid sorption systems.

2.8.1. Langmuir isotherm

The theoretical Langmuir isotherm is valid for adsorption of a solute from a liquid solution as monolayer adsorption on a surface containing a finite number of identical sites. Langmuir isotherm model assumes uniform energies of adsorption onto the surface without transmigration of adsorbate in the plane of the surface [18]. Therefore, the Langmuir isotherm model was chosen for the estimation of the maximum adsorption capacity corresponding to complete monolayer coverage on the adsorbent surface. The Langmuir equation is commonly expressed as follows:

$$\frac{C_e}{q_e}=\frac{1}{K_L\times q_{\max}}+\frac{C_e}{q_{\max}} \tag{1}$$

where q_e is monolayer adsorption capacity (mg/g), K_L is Langmuir isotherm constant related to the affinity of the binding sites and energy of adsorption (L/mg). The values of q_e and K_L can be calculated by plotting C_e/q_e vs. C_e (Fig. 11). The essential characteristics of a Langmuir isotherm can be expressed in terms of a dimensionless constant separation factor or equilibrium parameter, R_L, which is defined by $R_L = 1/(1 + K_L C_e)$. The influence C_e of isotherm shape on "favorable" or "unfavorable" adsorption has been considered. The R_L values indicate the type of the isotherm to be either unfavorable ($R_L > 1$), linear ($R_L = 1$), favorable ($0 < R_L < 1$), or irreversible ($R_L = 0$). In the present experiment, the results were found for R_L between 0.999 which clearly indicate the adsorption was favorable with CNT-ABS and results are shown in Table 1.

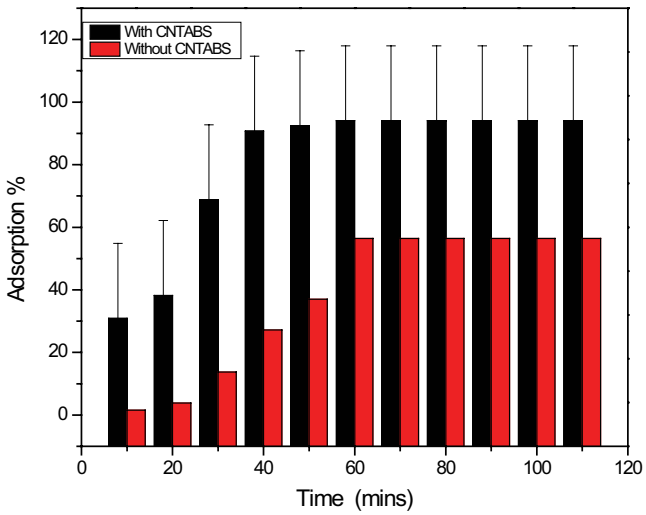

Fig. 8. Effect of contact time on malachite green dye adsorption.

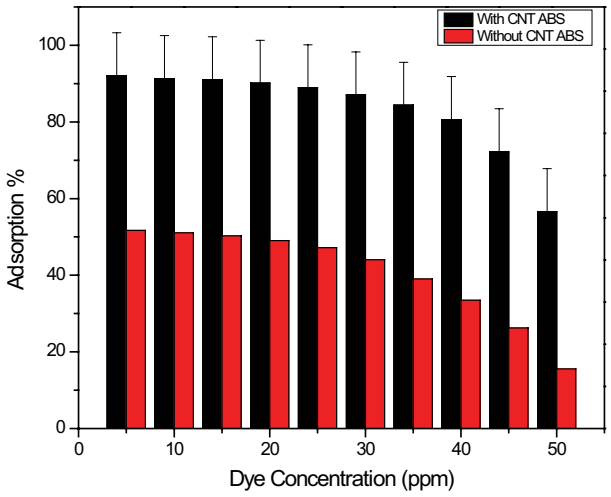

Fig. 9. Effect of initial concentration on malachite green dye adsorption.

2.8.2. Freundlich isotherm

The Freundlich equation was assigned for the adsorption of MG dye on the adsorbent. The Freundlich isotherm was expressed as:

$$\ln q_e = \ln K_F + \frac{1}{n}\ln C_e \tag{2}$$

The values of K_F show the Freundlich isotherm constant, n is the Freundlich component. Where q_e is the standard adsorption mass, C_e is the equilibrium concentration. Freundlich isotherm is an actual relation between the concentrations of solute on the surface of an adsorbent to the concentration of the solute in the liquid which is in contact [19]. Fig. 12 shows Freundlich isotherm of adsorption. The obtained R^2 values are summarised in Table 1.

2.8.3. Temkin isotherm

The Temkin isotherm accepts linear form rather than logarithmic form in decrease of heat of adsorption applicable to moderate concentration. It also assumes uniform distribution of bounding energy up to some maximum bonding energy [20]. The Tempkin isotherm was symbolized by:

$$q_e = B\ \ln A_T + B\ \ln C_e \tag{3}$$

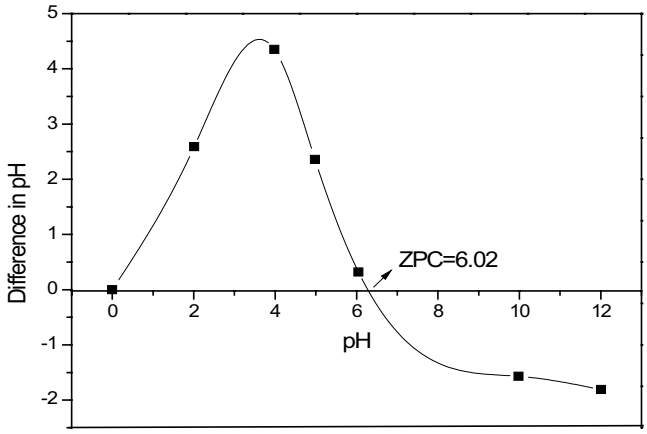

Fig. 10. Zero point charge measurement of titanium coated graphite with CNT-ABS.

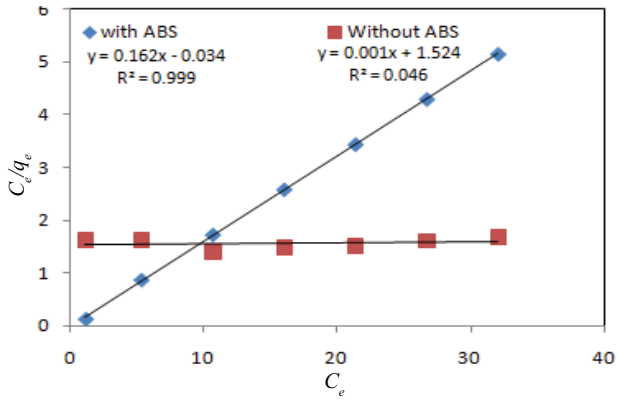

Fig. 11. Langmuir isotherm.

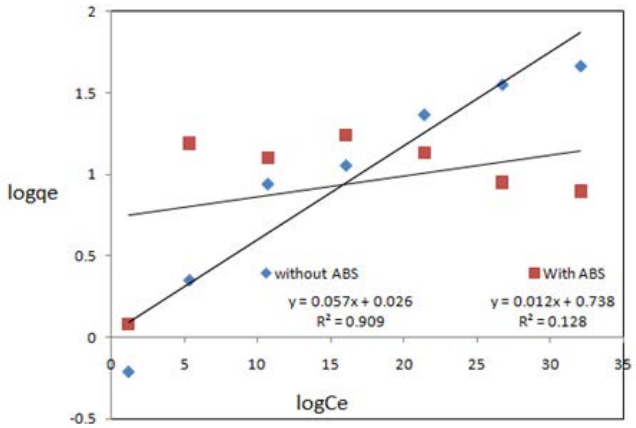

Fig. 12. Freundlich isotherm.

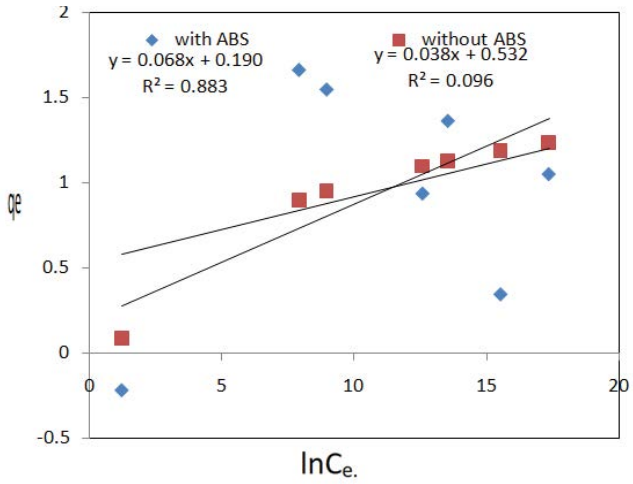

Fig. 13. Temkin isotherm.

where A_T is the Temkin isotherm equilibrium binding constant (L/g), b_T is the Temkin isotherm constant, R is the universal gas constant (8.314 J/mol/K), T is the temperature at 298 K. B is the constant related to heat of sorption (J/mol). From the Temkin plot shown in Fig. 13, the following values were estimated: A_T = 1.075 L/g, B = 25.34 J/mol which is an indication of the heat of sorption indicating a physical adsorption process, and the graph was carried out by plotting the quantity sorbed q_e against lnC_e.

The application of the Langmuir, Freundlich, and Temkin equation to the experimental data showed that the Langmuir model fitted well with the experimental data (R^2 = 0.999) than Freundlich model (R^2 = 0.909) and Temkin model (R^2 = 0.883) in case of Titanium coated on a graphite with CNT-ABS. Without the CNT-ABS all the model were not suitable for adsorption process. On this basis, also one would conclude that it was chemisorption. All these values are summarized in Table 1.

2.9. Kinetic study of adsorption

The kinetics of malachite green dye adsorption is necessary for choosing the optimum operating conditions, for the extensive batch process. The kinetic parameters, which are supportive for analyzing of adsorption rate, give information for designing and creating the adsorption processes. In order to enquire the mechanism of adsorption, different kinetic models have been recommended. Recently, adsorption mechanisms relating kinetics-based models have been published and calculated as per the literature [21]. In this study, two of the well-known models were investigated to find the best-fitted model for the experimental data obtained. The kinetic data were treated with the following pseudo-first-order rate equation.

$$\log\left(q_e - q_t\right) = \log q_e - \frac{k_1 t}{2.303} \tag{4}$$

where q_t and q_e are the amount adsorbed at time t and at equilibrium (mg/g) and k_1 is the pseudo-first-order rate constant for the adsorption process (1/min).

The pseudo-second-order model can be represented in the following form.

$$\frac{t}{q_t} = \frac{1}{k_2 q_e^2} + \left(\frac{1}{q_e}\right)t \tag{5}$$

where k_2 is the pseudo-second-order rate constant (g/mg min). The plots of log($q_e - q_t$) vs. t and the plots of t/q_t vs. t are shown in, respectively. Kinetic constants calculated from the graph of the both pseudo-first-order and pseudo-second-order plots show that pseudo-first-order is fitted better than pseudo-second-order and results are given in Table 2.

2.10. Mechanism of adsorption

Stronger adsorption ability is one of the characteristics of polar organic dye, and it is easily adsorbing on the large specific surface area of CNT. Three steps are involved in the removal of dye by titanium coated graphite with CNT-ABS nanocomposite. In the first step, the malachite green dye molecules migrated from the bulk liquid phase to the outer surface of adsorbent particles. In the second step, the malachite green dye molecules moved within the pores of adsorbent particles. In the third step, the adsorption of malachite green dye molecules by titanium coated

Table 1
Adsorption isotherm

Titanium coated on a graphite	Langmuir model		Freundlich model		Tempkin model	
	With CNT-ABS	Without CNT-ABS	With CNT-ABS	Without CNT-ABS	With CNT-ABS	Without CNT-ABS
	R^2	R^2	R^2	R^2	R^2	R^2
	0.999	0.046	0.909	0.128	0.883	0.096

Table 2
Kinetics of malachite green dye adsorption

Pseudo-first-order		Pseudo-second-order	
With CNT-ABS	Without CNT-ABS	With CNT-ABS	Without CNT-ABS
R^2	R^2	R^2	R^2
0.995	0.717	0.935	0.358

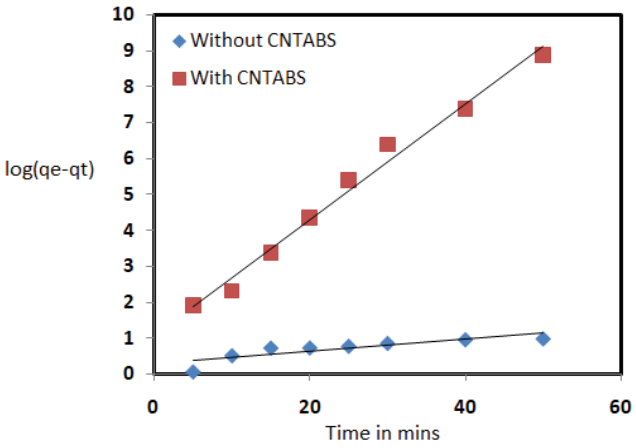

Fig. 14. Pseudo-first-order model.

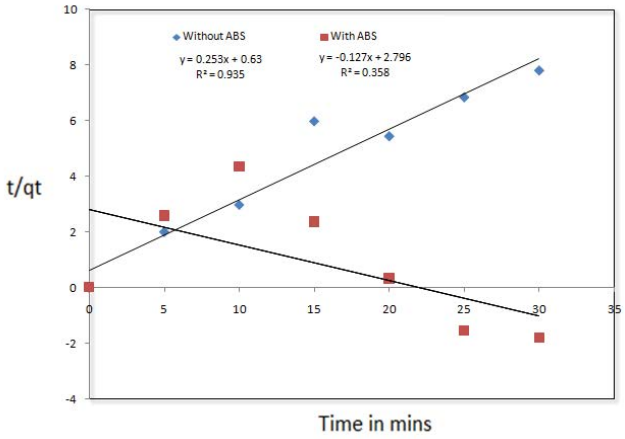

Fig. 15. Pseudo-second-order model.

graphite with CNT-ABS nanocomposite took place on the surface. As per the isothermal studies, it is a chemisorption process. In this chemisorption process, the cationic dyes showed a high affinity to be adsorbed on CNT; this fact could be attributed to the electrostatic interactions between π-electrons of CNT and the positively charged moieties of the cationic dyes. This phenomenon was referred to as π–π electron-donor (CNT)/acceptor (cationic dyes) interaction.) among the cationic dyes, MG is an ideally planar molecule and therefore could be easily adsorbed by π–π interactions [22] between the aromatic backbone of the dyes and CNT. Thus, titanium coated graphite with CNT-ABS nanocomposite was expected to play a promising role in the field of organic pollutant removal.

3. Regeneration and reusability

Thus, we have seen that the adsorption process is a simple and cheapest process. In this regard, the regeneration of the material and reusability is very important aspect. In order to check the reusability, the synthesized titanium

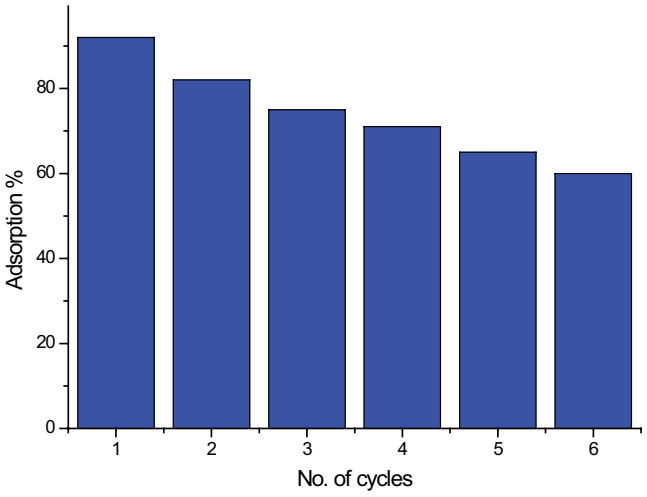

Fig. 16. Percentage removal of Malachite green dye for regenerated adsorbent at different cycle runs.

coated graphite with CNT-ABS nanomaterial was taken in a beaker and adsorption was allowed to take place in the presence of Malachite green dye and the mixture was stirred well for around 60 min. After the adsorption process is over, the spent adsorbent was filtered and was washed with deionized water. The filter paper was heated about 150°C in order to remove all the adsorbed dye and also to restore the adsorbent sites and to reactivate the adsorbent. Regeneration experiment was repeated for six more cycles by stirring the adsorbent with Malachite green dye for 60 min under the similar previous condition and the absorbance of the compound was measured each cycle. The results are shown in Fig. 16. Which shows that for the regeneration the adsorbent efficiency has decreased to 92% after the first recycling, may be due to the clustering of nanoparticles on sintering. But, for further cycles the % decrease in efficiency was more or less linear decreasing order. Thus, this material can be efficiently reused for many cycles for the purification/adsorption process.

4. Conclusion

In this paper, titanium coated graphite CNT-ABS nanocomposite and titanium coated graphite was proposed and its dye removal ability was evaluated and compared. It was observed that titanium coated graphite CNT-ABS nanocomposite gives better dye adsorption efficiency and has advantages over titanium coated graphite. Malachite green dye was used as a standard toxic dye. Adsorption kinetic of dye was found to confirm to pseudo-first-order kinetics. It was found that dye adsorption onto the electroless titanium coated graphite with CNT-ABS nanocomposite followed with Langmuir isotherm. It can be decided that the electroless titanium coated graphite CNT-ABS nanocomposite being as an adsorbent with high dye adsorption capability could be an acceptable substitute to remove dyes from colored aqueous solutions.

Author contributions

UJ (Ph.D. student) contributed in collecting the samples, running the laboratory work, drafted the paper. DB analyzed the data and redrafted the paper. BN contributed the critical reading of the manuscript. All the authors have read the final manuscript and approved for the submission.

References

[1] A.R. Shawwa, D.W. Smith, D.C. Sego, Color and chlorinated organics removal from pulp mills wastewater using activated petroleum coke, Water Res., 35 (2001)745–749.
[2] C. Hachem, F. Bocquillon, O. Zahraa, M. Bouchy, Decolorization of textile industry wastewater by the photocatalytic degradation process, Dyes Pigm., 49 (2001) 117–125.
[3] B. Sharma, A.K. Dangi, P. Shukla, Contemporary enzyme based technologies for bioremediation: a review, J. Environ. Manage., 210 (2018) 10–22.
[4] G. Sudarjanto, B. Keller-Lehmann, J. Keller, Optimization of integrated chemical–biological degradation of a reactive azo dye using response surface methodology, J. Hazard. Mater., 138 (2006) 160–168.
[5] X.T. Liu, M.S. Wang, S.J. Zhang, B.C. Pan, Application potential of carbon nanotubes in water treatment: a review, J. Environ. Sci., 25 (2013) 1263–1280.
[6] M.A. Shannon, P.W. Bohn, M. Elimelech, J.G. Georgiadis, B.J. Marinas, A.M. Mayes, Science and technology for water purification in the coming decades, J. Nanosci. Nanotechnol., 452 (2010) 337–346.
[7] X.J. Peng, Y.H. Li, Z.K. Luan, Z.C. Di, H.Y. Wang, B.H. Tian, Z.P. Jia, Adsorption of 1,2-dichlorobenzene from water to carbon nanotubes, Chem. Phys. Lett., 376 (2003) 154–158.
[8] S. Arivoli, M. Hema, P.M. Prasath, Adsorption of malachite green onto carbon prepared from borassus bark, Arabian J. Sci. Eng., 34 (2009) 31–42.
[9] B.M. Vanderborght, R.E. Van Grieken, Enrichment of trace metals in water by adsorption on activated carbon, Anal. Chem., 49 (1977) 311–316.
[10] K. Saeed, I. Khan, Carbon nanotubes–properties and applications: a review, Carbon Lett., 14 (2013)131–144.
[11] M.S. Mauter, M. Elimelech, Environmental applications of carbon-based nanomaterials, Environ. Sci. Technol., 42 (2008) 5843–5859.
[12] X.M. Zhang, H.W. Yu, H.J. Yang, Y.C. Wan, H. Hu, Z. Zhai, J.M. Qin, Graphene oxide caged in cellulose microbeads for removal of malachite green dye from aqueous solution, J. Colloid Interface Sci., 437 (2015) 277–282.
[13] K.S. Jithendra kumara, G. Krishnamurthy,B.E. Kumara Swamy, N.D. Shashi kumar, S. Naik, B.S. Krishna, N. Naik, Terephthalic acid derived ligand-stabilized palladium nanocomposite catalyst for Heck coupling reaction: without surface-modified heterogeneous catalyst, Appl. Organomet. Chem., 31 (2017), doi: 10.1002/aoc.3549.
[14] D.Y. Zhang, Removal of malachite green from water by Firmiana simplex wood fiber, Electron. J. Biotechnol., 12 (2009) 9–10.
[15] S. Sartape, A.M. Mandhare, V.V. Jadhav, P.D. Raut, M.A. Anuse, S.S. Kolekar, Removal of malachite green dye from aqueous solution with adsorption technique using *Limonia acidissima* (wood apple) shell as low cost adsorbent, Arabian J. Chem., 10 (2017) S3229–S3238.
[16] E.J. Lara-Vásqueza, M. Solache-Ríosb, E. Gutiérrez-Seguraa, Malachite green dye behaviors in the presence of biosorbents from maize (*Zea mays* L.), their Fe-Cu nanoparticles composites and Fe-Cu nanoparticles, J. Environ. Chem. Eng., 4 (2016) 1594–1603.
[17] M. Rajabi, K. Mahanpoor, O. Moradi, Removal of dye molecules from aqueous solution by carbon nanotubes and carbon nanotube functional groups: critical review, RSC Adv., 7 (2017) 47083–47090.
[18] F.E. Titchou, R.A. Akbour, A. Assabbane, M. Hamdani, Removal of cationic dye from aqueous solution using *Moroccan pozzolana* as adsorbent: isotherms, kinetic studies, and application on real textile wastewater treatment, Groundwater Sustainable Dev., 11 (2020) 100405.
[19] U. Jinendra, D. Bilehal, B.M. Nagabhushana, K. Raghava Reddy, Ch. Venkata Reddy, A.V. Raghu, Template-free hydrothermal synthesis of hexa ferrite nanoparticles and its adsorption capability for different organic dyes: comparative adsorption studies, isotherms and kinetic studies, Mater. Sci. Energy Technol., 2 (2019) 657–666.
[20] A.A. Inyinbor, F.A. Adekola, G.A. Olatunji, Kinetics, isotherms and thermodynamic modeling of liquid phase adsorption of Rhodamine B dye onto *Raphia hookerie* fruit epicarp, Water Resour. Ind., 15 (2016) 14–27.
[21] S. Zhang, T. Shao, H.S. Kose, T. Karanfil, Adsorption kinetics of aromatic compounds on carbon nanotubes and activated carbons, Environ. Toxicol. Chem., 31 (2012) 79–85.
[22] E.M. Pérez, N. Martín, π–π interactions in carbon nanostructures, Chem. Soc. Rev., 44 (2015) 6425–6433.